Chapter 13

The Fermi Surfaces

Chapter Outline

13.1 CONSTANT ENERGY SURFACES

The locus of all the points at which the energy $E_{\mathbf{k}}$ has a constant value is called a constant energy surface. The shape of the constant energy surface depends on the nature of the energy bands. One can define any number of constant energy surfaces for different values of $E_{\mathbf{k}}$. In a one-dimensional free-electron gas the energy bands are parabolic in nature and are given by

$$E_{\mathbf{k}} = \frac{\hbar^2 k^2}{2m_e} \tag{13.1}$$

In this case one can define points with constant energy and Fig. 13.1A shows two equidistant points with constant energy $E_{\mathbf{k}}$. In a two-dimensional solid, one can define constant energy contours. Fig. 13.1B shows *circles* as the constant energy contours in a two-dimensional free-electron gas. But in a three-dimensional solid one can define constant energy surfaces. In a three-dimensional free-electron gas, the energy bands are parabolic, just as defined by Eq. (13.1), and they yield spherical constant energy surfaces (see Fig. 13.1C).

13.2 THE FERMI SURFACES

The Fermi surface (FS) is a special constant energy surface and is defined as the locus of all of the points at which the value of energy is E_F. In the preceding chapters, we have discussed the fact that it is the electron states very near the FS that determine most of the electronic properties of crystalline solids. This is because the electrons in these states can be easily excited to the vacant states above the FS by the application of a small external field. Hence the nature of energy bands in the neighborhood of the FS is of primary importance and requires our special attention.

13.3 THE FERMI SURFACE IN THE FREE-ELECTRON APPROXIMATION

In a one-dimensional free-electron gas, the Fermi energy is given by (Eq. 9.50)

$$E_F = \frac{\hbar^2 k_F^2}{2m_e} = \frac{\pi^2 \hbar^2 n_e^2}{2m_e} \tag{13.2}$$

where n_e is the linear density of electrons. The points at which energy has value E_F are equidistant from the center of the 1BZ and are symmetrically spaced on both sides of it (see Fig. 13.1A). In a two-dimensional free-electron gas the Fermi energy is given by (see Eq. 9.41)

Solid State Physics. https://doi.org/10.1016/B978-0-12-817103-5.00013-X

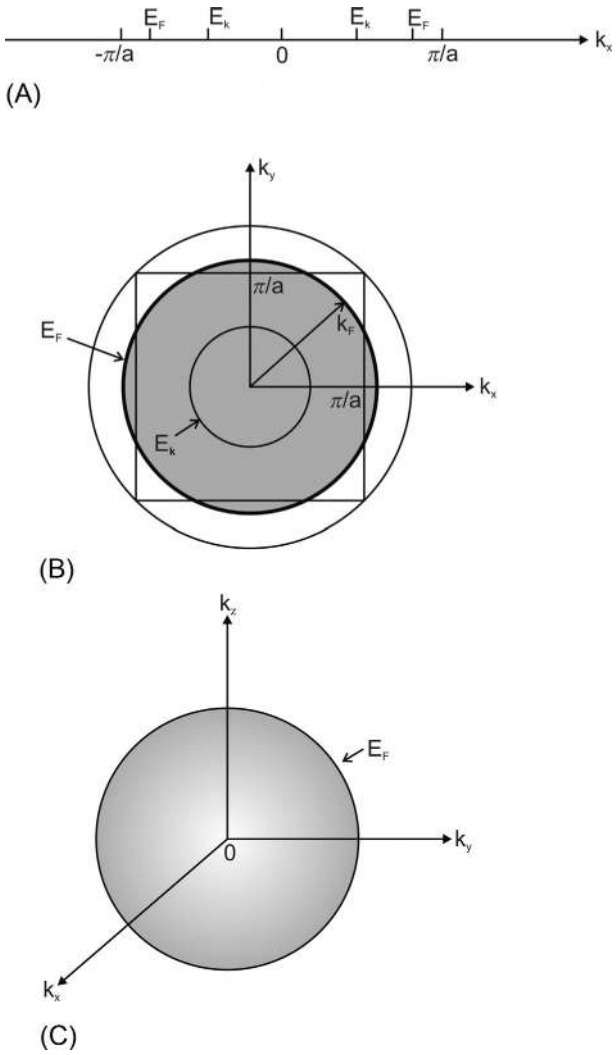

FIG. 13.1 (A) Two points having constant energy E_k in a one-dimensional free-electron gas. The figure also shows two points having Fermi energy E_F lying within the 1BZ. (B) The constant energy circular contours with different values of energy $E_{\mathbf{k}}$ in the square lattice of a two-dimensional free-electron gas. The figure also shows the circular contour having Fermi energy E_F. (C) The spherical Fermi surface with constant energy E_F in a three-dimensional free-electron gas.

$$E_F = \frac{\hbar^2 k_F^2}{2m_e} = \frac{\pi \hbar^2 n_e}{m_e} \tag{13.3}$$

where n_e is the surface electron density. The Fermi circle with its center as the center of the 1BZ and radius k_F is shown in Fig. 13.1B. In the three-dimensional free-electron gas the Fermi energy, from Eqs. (9.16), (9.19), is given by

$$E_F = \frac{\hbar^2}{2m_e}\left(3\pi^2 \frac{Z}{V_0}\right)^{2/3} \tag{13.4}$$

The components of the wave vector **k** at the 1BZ boundary are given by

$$k_X = k_y = k_Z = \pm\frac{\pi}{a} \tag{13.5}$$

The FS is a sphere with radius k_F having center at the center of the 1BZ of the lattice and is shown in Fig. 13.1C. In the free-electron approximation, three distinct classes of the Fermi surface are observed.

13.3.1 Type I Fermi Surface

It is evident from Eq. (13.4) that in the free-electron approximation, the value of k_F depends upon the electron concentration. In solids with a low electron concentration, the entire FS may lie in the 1BZ. In this case, only the first band (which

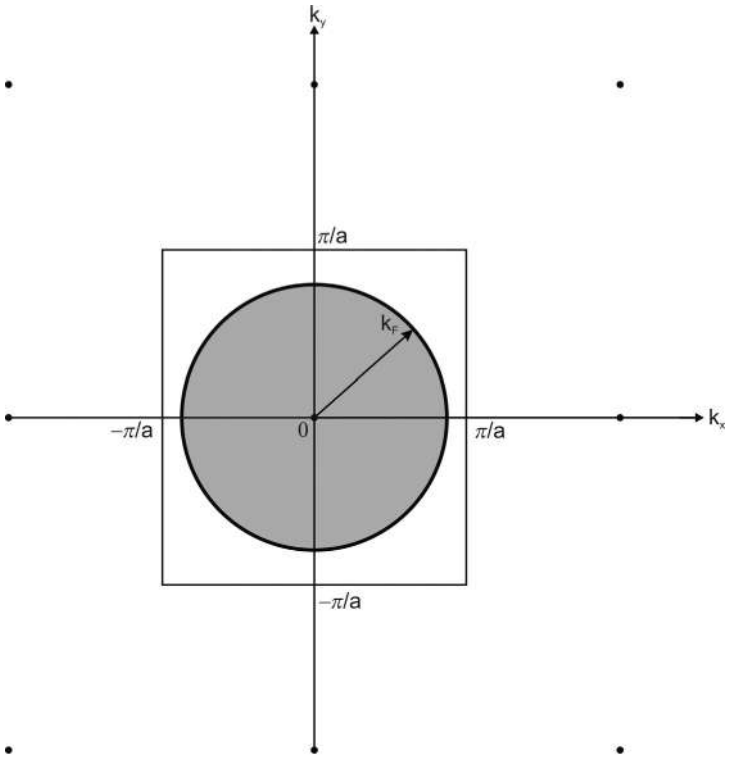

FIG. 13.2 The Fermi circle of a gas of low-electron-density free electrons in a square lattice. The *dots* represent the lattice points in the reciprocal lattice of a square lattice with periodicity a. The 1BZ is a square with side $2\pi/a$.

lies in the 1BZ) is partially filled, the others are empty. Fig. 13.2 shows, for simplicity, a circular FS for a two-dimensional square lattice with low electron density.

13.3.2 Type II Fermi Surface

In crystalline solids with a reasonably large concentration of electrons, the FS may extend to the higher order BZs. Fig. 13.3A shows the FS of a square lattice, which extends to the 2BZ. Here the FS exhibits two partially filled bands: the first band lies in the 1BZ and the second in the 2BZ. It has already been discussed that all of the significant values of **k** lie in the 1BZ. Therefore, it is the usual practice to reduce the FS to the 1BZ (reduced zone scheme).

Fig. 13.3B and C shows the first and second bands in the reduced zone scheme, that is, in the 1BZ. Fig. 13.4A and B shows the first and second bands of the square lattice in the periodic zone scheme, which are repeated periodically. From Fig. 13.4A it is evident that the FS for the first band consists of pockets of holes at the corners of the 1BZ, while the FS of the second band (Fig. 13.4B) exhibits electron pockets at the middle of the sides of the 1BZ. It should be noted that both the bands in Fig. 13.4 are plotted in the 1BZ and the pieces of the FS that stick out of the zone must be interpreted in the periodic zone scheme.

13.3.2.1 Electron Orbits

For a changing electron state, the **k** point with a particular energy changes its position with time. The closed path of the **k** point in the reciprocal space is called an *orbit* and the periodic zone scheme is more suitable (not essential) for its representation. It is of particular interest to consider orbits along which the energy is constant and has a value equal to E_F. These orbits provide very useful information about the shape of the FS as they lie on the FS. Moreover, such orbits are experimentally accessible. In two-dimensional crystals such orbits just coincide with the FS itself. Fig. 13.5A shows the part of the FS for the first energy band in the 1BZ of a two-dimensional electron gas. The orbit corresponding to the hole pockets of the first band in the reduced zone scheme is a discontinuous one. The motion of an electron in this orbit can be described as follows:

1. Let an electron start from the state represented by point A and go from state A to state B. The electron is then Bragg reflected at B and goes to state C. The state C is identical to the state B as it differs from state B by a reciprocal lattice vector, $\mathbf{k} = \mathbf{G}$.

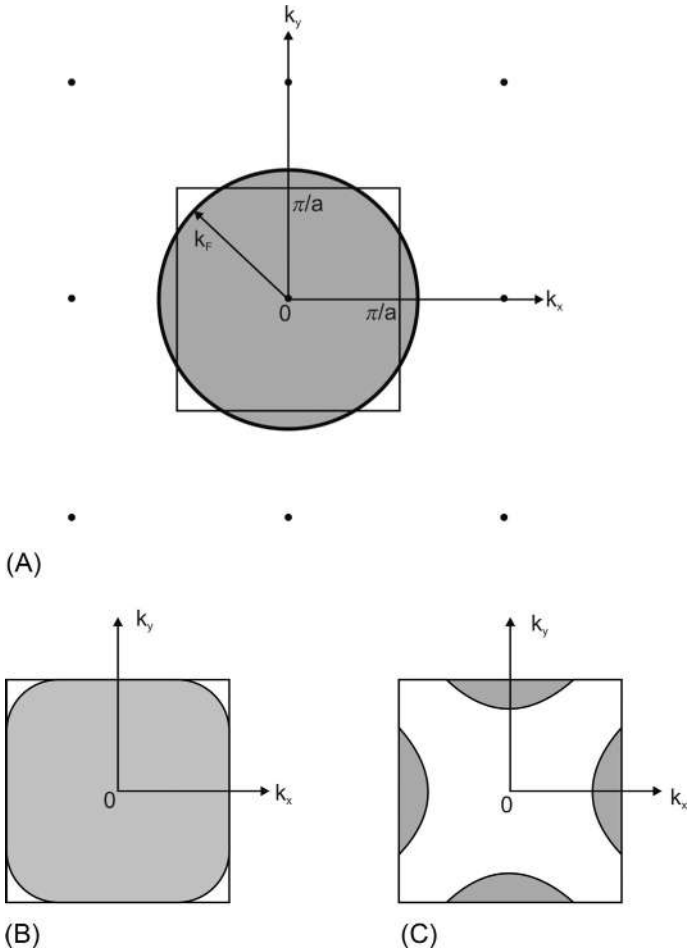

FIG. 13.3 (A) The Fermi surface extending to the 2BZ in the square lattice of a two-dimensional free-electron gas with reasonably large electron density. (B) The Fermi surface of the first energy band in the 1BZ of a two-dimensional free-electron gas. (C) The Fermi surface of the second energy band reduced to the 1BZ in a two-dimensional free-electron gas.

2. The electron goes from state C to state D and is then Bragg reflected at D and goes to state E.
3. The electron from state E goes to state F and is then Bragg reflected at F and goes to state G.
4. Finally, the electron moves from state G to state H and is then Bragg reflected from here to state A.

The same process can be shown in the periodic zone scheme in which the hole orbit is a continuous one (see Fig. 13.5B). The reader is also referred to Fig. 13.4A. It is evident that the continuous orbits in the periodic zone scheme are more appealing and easier to understand than the discontinuous orbits in the reduced zone scheme.

Fig. 13.6A and B shows the electron orbits for the second band in the reduced zone and periodic zone schemes. Again, the discontinuous orbit in the reduced zone scheme can be visualized as a continuous electron orbit in the periodic zone scheme. Further, the representation of the electron pockets (situated at the midpoint of each side of the 1BZ) is more appealing in the periodic zone scheme (also see Fig. 13.4B).

13.3.3 Type III Fermi Surface

In crystalline solids with higher electron concentration, the FS may extend to the higher order BZs. Fig. 13.7A shows a square lattice in **k**-space with its FS extending to the 4BZ. The portions of the FS in the 1BZ, 2BZ, 3BZ, and 4BZ, which show, respectively, the FS sections due to the first, second, third, and fourth bands, can be reduced to the 1BZ (Fig. 13.7B). It is evident that the FS due to the second band exhibits the orbit of a hole pocket around the center of the 1BZ. The FS corresponding to the third and fourth bands is disconnected in the reduced zone scheme. The discontinuous electron orbits for the third and fourth energy bands, in the reduced zone scheme, are shown in Fig. 13.8.

Any band can be plotted in the periodic zone scheme by translating its plot in the reduced zone scheme by all possible reciprocal lattice vectors. The plot of the second band and its hole orbit in the periodic zone scheme remain the same, as shown in Fig. 13.7B. Plots of the third and fourth bands are shown in Fig. 13.9, in which the discontinuous electron orbits

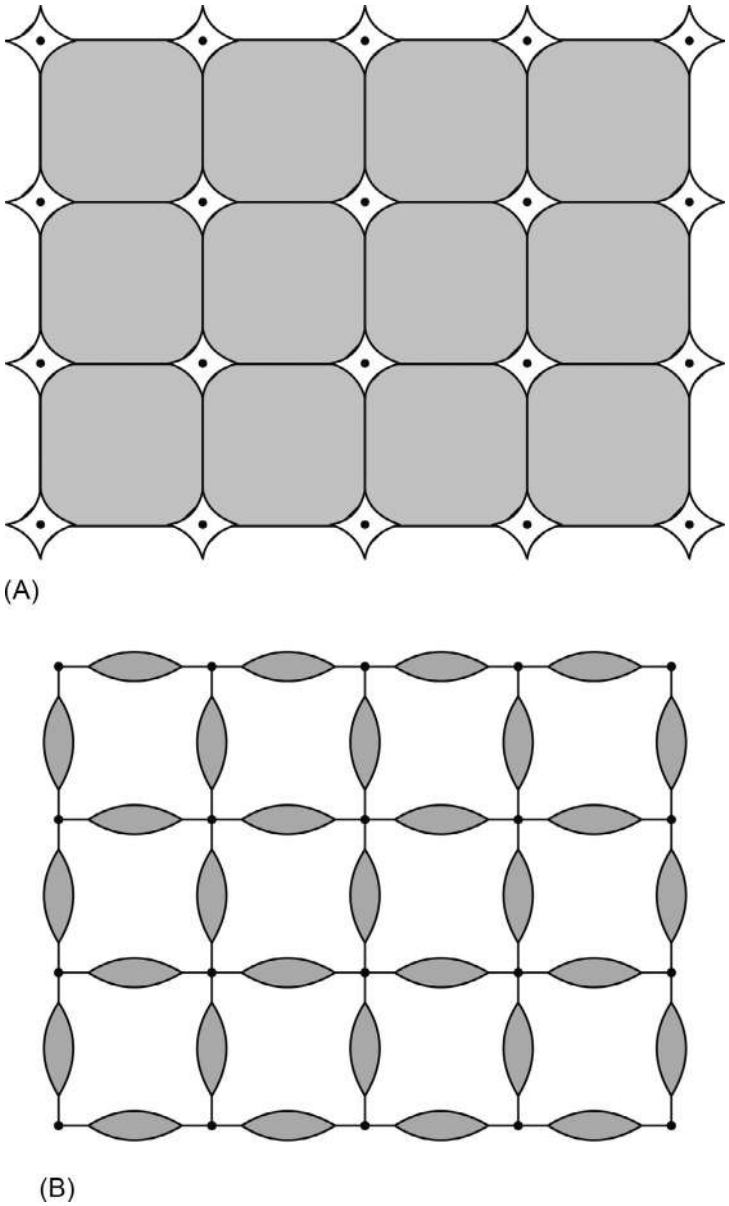

FIG. 13.4 The Fermi surface of the (A) first and (B) second energy bands in the periodic zone scheme in a two-dimensional free-electron gas having a square lattice.

are represented by continuous electron orbits. The third and fourth band Fermi surfaces exhibit electron pockets centered at the corners of the 1BZ. It is noteworthy that the hole orbit corresponding to the second band FS is continuous, even in the reduced band scheme, in contrast to the third and fourth band FS sections.

13.4 HARRISON'S CONSTRUCTION OF THE FERMI SURFACE

Harrison (1960) gave an elegant method for the construction of an FS corresponding to different bands of a crystalline solid in the periodic zone scheme. In this method, the reciprocal lattice corresponding to the crystal structure is determined and the free electron Fermi sphere is drawn around each lattice point. The problem is how to assign the various segments to the bands. Within each Fermi sphere all the states are occupied, while the states are empty outside. Now if some point, in the reduced zone scheme, lies within n spheres, then there are n occupied energy bands at that point in the reduced zone scheme and these bands are ordered in increasing energy. Therefore, the spherical segments, which separate regions of the reduced zone within n spheres from regions within (n + 1) spheres are segments of the FS arising from the nth band, that is, these

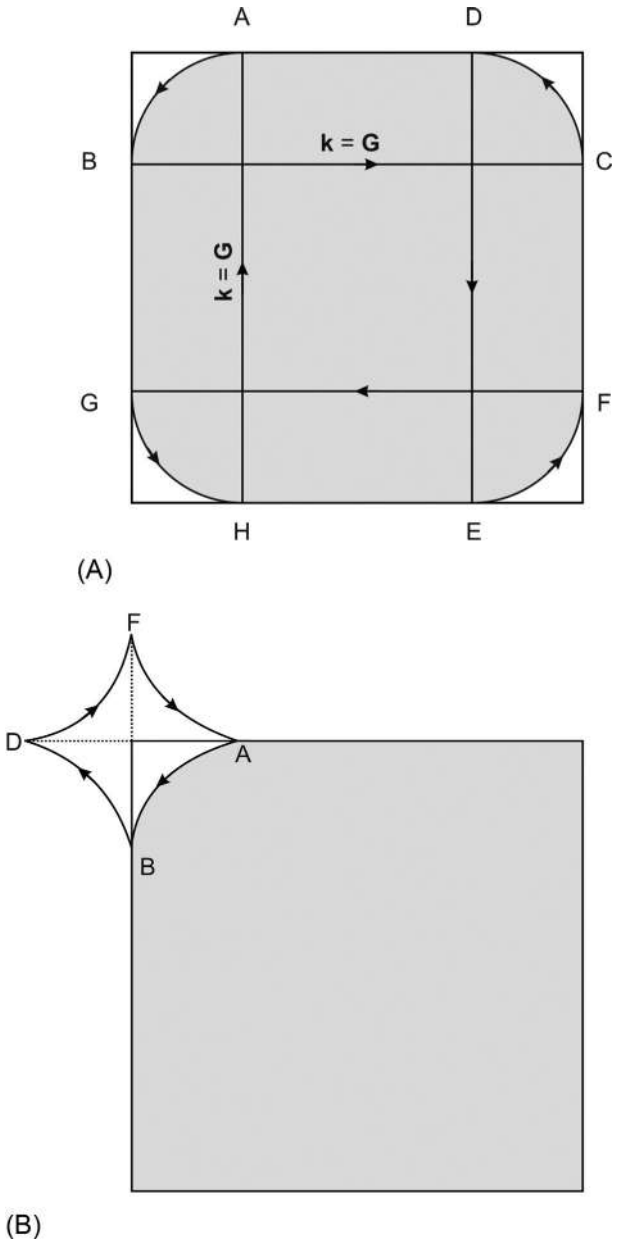

FIG. 13.5 (A) The discontinuous hole orbit of the first band in the 1BZ of a square lattice in a two-dimensional free-electron gas. (B) The continuous hole orbit of the first band in the periodic zone scheme of a square lattice in a two-dimensional free-electron gas.

segments separate occupied regions from unoccupied ones in the nth band. For example, points in the reciprocal space that lie within at least one sphere correspond to occupied states in the first zone (1st band). Points within at least two spheres correspond to occupied states in the second zone (2nd band), with similar results for points in three or more spheres. Hence, the construction of the FS arising from the various bands is reduced to the construction of Fermi spheres and counting them at a particular point or region.

Fig. 13.10 shows Harrison's construction of the FS for a square lattice in the free-electron approximation when the Fermi sphere extends to the 4BZ. It shows the second, third, and fourth bands in the periodic zone scheme. Here the 1BZ has been constructed in two ways. The first is the usual 1BZ, which contains one lattice point at its center and is called the 1BZ of type (a) for convenience. The second construction of the 1BZ has lattice points at the corners and is called the 1BZ of type (b). The first band fills the whole of the 1BZ. The FS of the second band in the 1BZ of type (a) represents a hole pocket with a lattice point at its center, while in the 1BZ of type (b) it consists of hole pockets at the corners of the 1BZ (see Fig. 13.10). The FS of the third band consists of four electron pockets, each at the corner of the 1BZ of type (a), but forming a rosette at the center of the 1BZ of type (b). The FS of the fourth band consists of four electron pockets at the corners of the

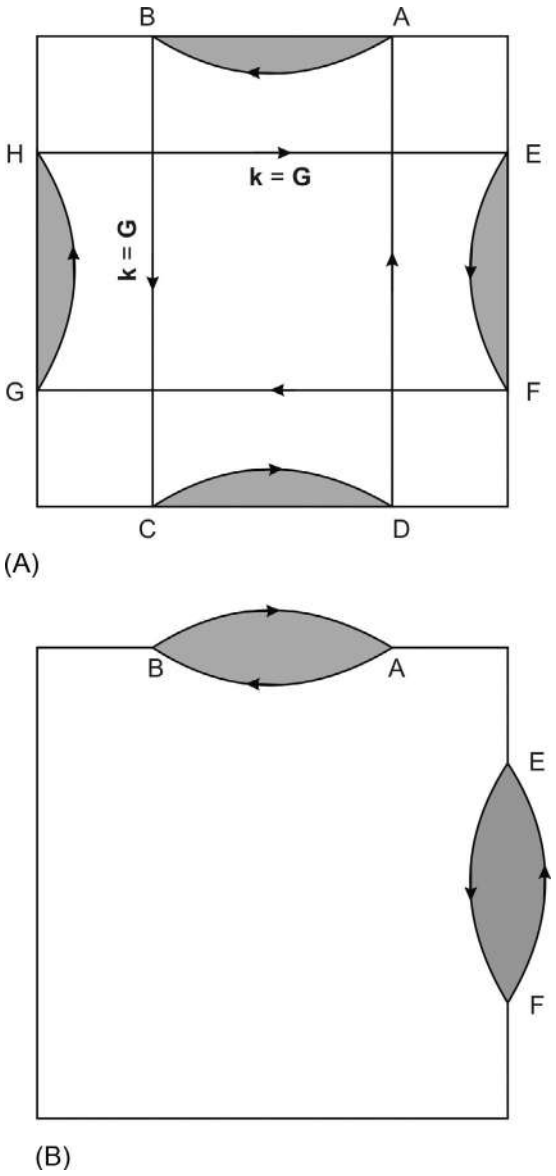

FIG. 13.6 (A) The discontinuous electron orbit of the second band, in the reduced zone scheme, of a square lattice in a two-dimensional free-electron gas. (B) The continuous electron orbit of the second band, in the periodic zone scheme, of a square lattice in a two-dimensional free-electron gas.

1BZ of type (a) but forms a single electron pocket at the center of the 1BZ of type (b). Fig. 13.11 shows the FS of the first four bands drawn in the 1BZ of type (a), while Fig. 13.12 shows the FS of the third and fourth bands drawn in the 1BZ of type (b). It is evident from Fig. 13.11 that one gets the same FS as shown in Fig. 13.7.

13.5 NEARLY FREE-ELECTRON APPROXIMATION

In the previous section the effect of the periodic lattice potential on the motion of an electron and on the FS has been neglected. In reality, an electron experiences the periodic potential of the lattice, which modifies its motion significantly, and hence modifies the electron energy bands and the Fermi surface in a crystalline solid. In Chapter 12, the nearly free-electron approximation, which yielded the lowest order improvement in the energy bands, was discussed. Therefore, it is worthwhile to construct the FS in this approximation and compare the results with those obtained in the free-electron approximation. In the nearly free-electron approximation the energy bands are modified as the zone boundary is reached in the following fashion:

1. The energy bands cut the BZ boundary in a perpendicular direction.
2. The bands exhibit an energy band gap at the zone boundary due to the rounding off of the energy bands.

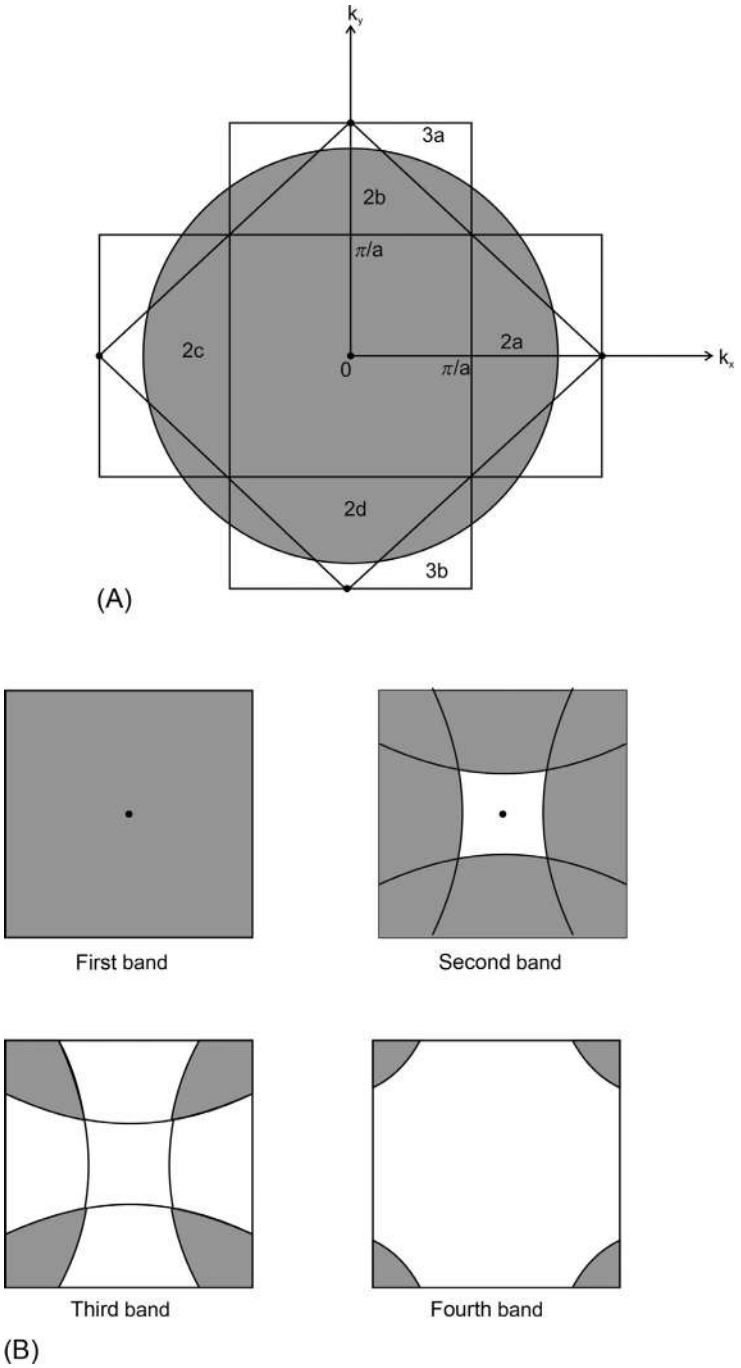

FIG. 13.7 (A) The Fermi surface extending up to the 4BZ of the square lattice in a two-dimensional free-electron gas. (B) The Fermi surfaces of the first four bands, in the reduced zone scheme, of a square lattice in a two-dimensional free-electron gas.

The FS in the nearly free-electron approximation, which extends to the 2BZ, is shown in Fig. 13.13. The FS in the reduced zone scheme is shown in Fig. 13.14 and in the periodic zone scheme in Fig. 13.15. A comparison of Figs. 13.4 and 13.15 shows that the Fermi surfaces for both the first and second bands, in the nearly free-electron approximation, are rounded off at the corners. Further, the FS intersects the BZ boundary in the perpendicular direction. It is noteworthy that the total volume enclosed by the FS depends only on the electron concentration and is independent of the details of the periodic potential.

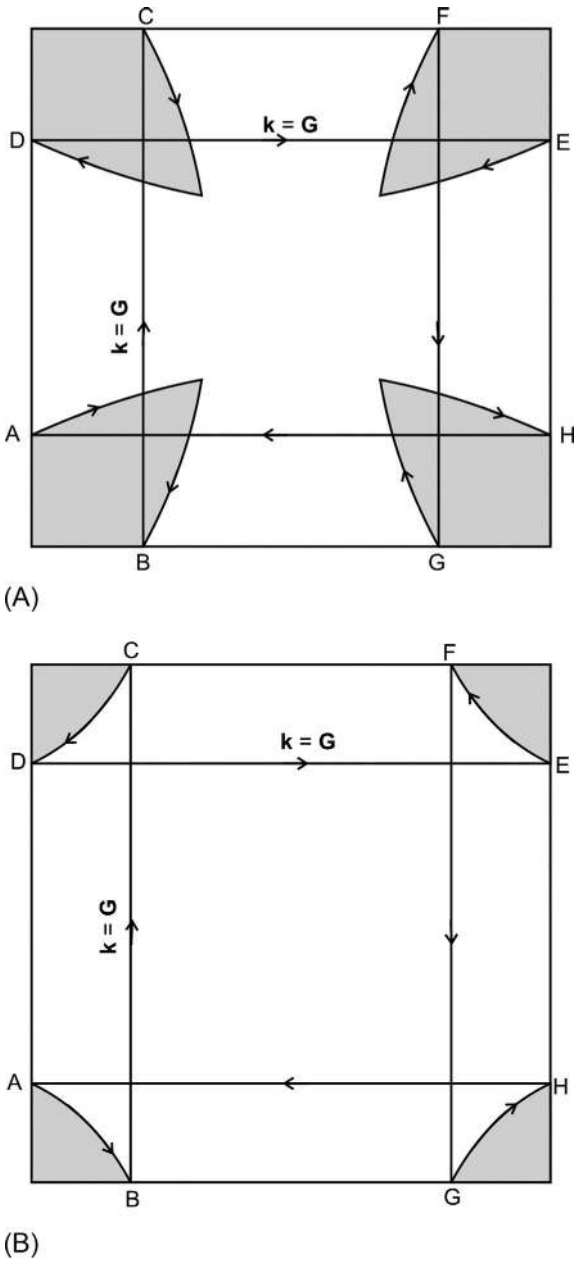

FIG. 13.8 The discontinuous electron orbits for the (A) third and (B) fourth bands, in the reduced zone scheme, of a square lattice in a free-electron gas.

13.6 THE ACTUAL FERMI SURFACES

Metal is a three-dimensional crystalline solid in which there can be more than one electron energy band lying on or crossing the FS. Each of these bands will yield a part of the FS, which separates the occupied states from the unoccupied ones. Here we shall consider only simple metals, which exhibit simple Fermi surfaces.

13.6.1 Monovalent Metals

Monovalent free-electron metals with conduction electrons possessing the s-character constitute the simplest of the metals: the alkali metals, such as Na and K, constitute such a category. Na metal has a bcc crystal structure with the 1NN distance as $\sqrt{3}a/2$ and the volume per atom $V_0 = a^3/2$. The reciprocal lattice of Na metal has fcc symmetry with the shortest reciprocal lattice vectors given by $(2\pi/a)(\pm 1, \pm 1, 0)$, $(2\pi/a)(\pm 1, 0, \pm 1)$, $(2\pi/a)(0, \pm 1, \pm 1)$. The boundary of the 1BZ is at a distance

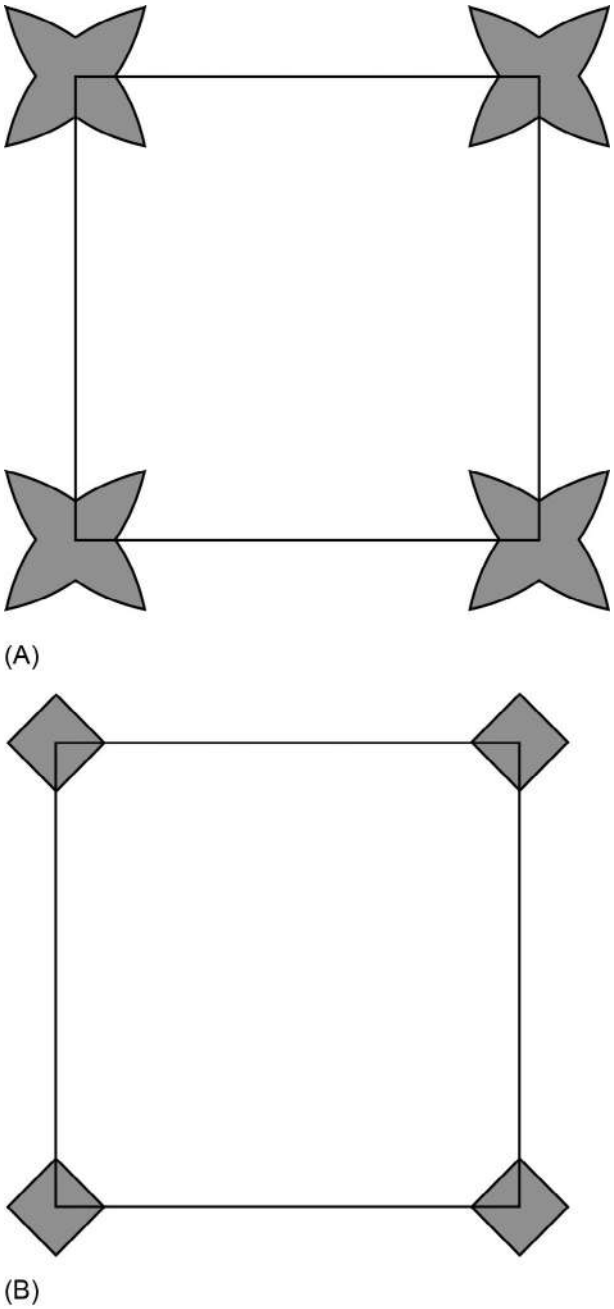

FIG. 13.9 The continuous electron orbits for the (A) third and (B) fourth bands, in the periodic zone scheme, of a square lattice in the free-electron approximation.

$d = \sqrt{2}\pi/a$, which is half of the distance of the 1NN in the reciprocal lattice. For a monovalent metal one can get from Eq. (9.19)

$$k_F = \left(\frac{3\pi^2}{V_0}\right)^{1/3} \tag{13.6}$$

For Na metal with a bcc structure one can write, from Eq. (13.6),

$$k_F = \frac{(6\pi^2)^{1/3}}{a} \tag{13.7}$$

Hence,

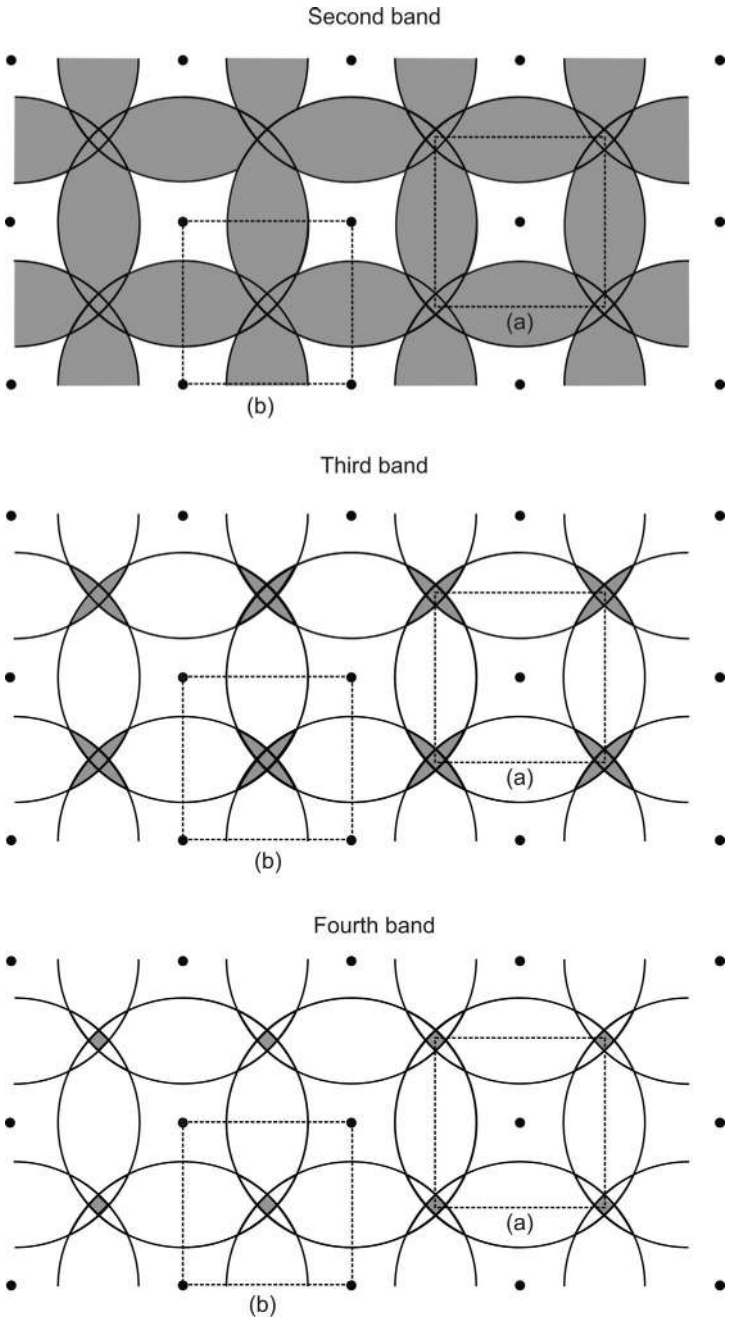

FIG. 13.10 Harrison's construction for the Fermi surface of the second, third, and fourth bands of a square lattice in a two-dimensional free-electron metal (the periodic zone scheme).

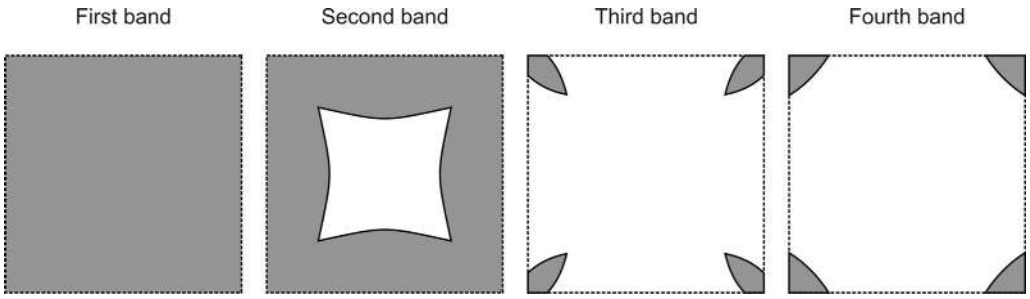

FIG. 13.11 The Fermi surfaces for the first four bands in the 1BZ of type (a) of the square lattice obtained from Harrison's construction in a free-electron metal (the reduced zone scheme).

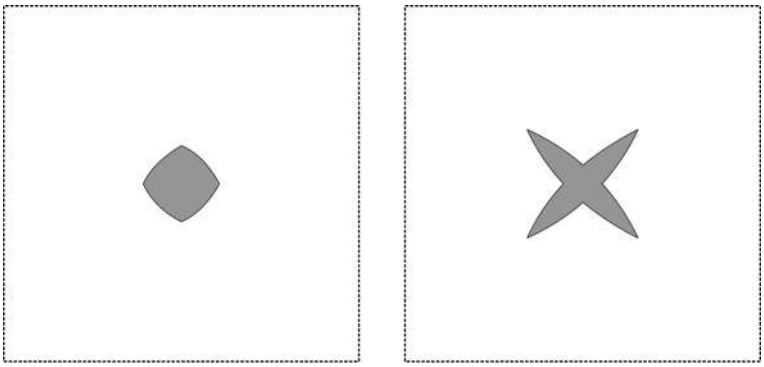

FIG. 13.12 The Fermi surfaces for the third and fourth bands in the 1BZ of type (b), obtained from Harrison's construction, which lie at the center of the 1BZ.

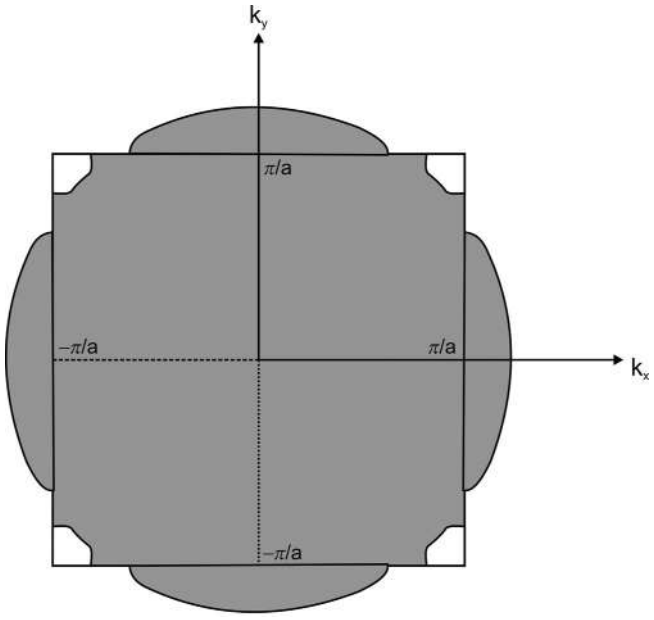

FIG. 13.13 The Fermi surface for a two-dimensional nearly free-electron metal with a square lattice that extends to the 2BZ.

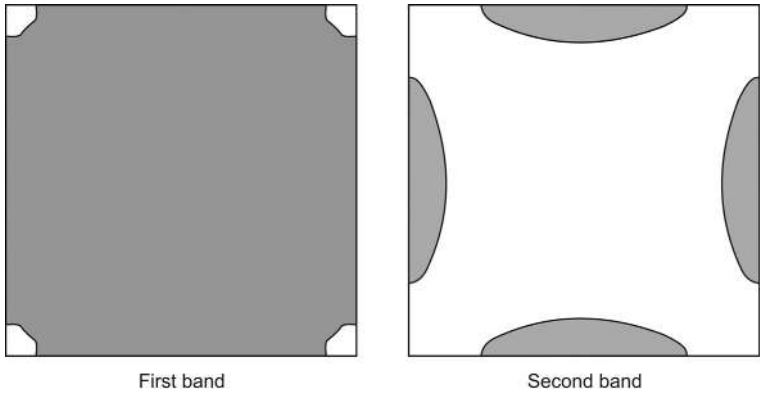

FIG. 13.14 The Fermi surface of the first and second energy bands in a square lattice for a two-dimensional nearly free-electron metal (the reduced zone scheme).

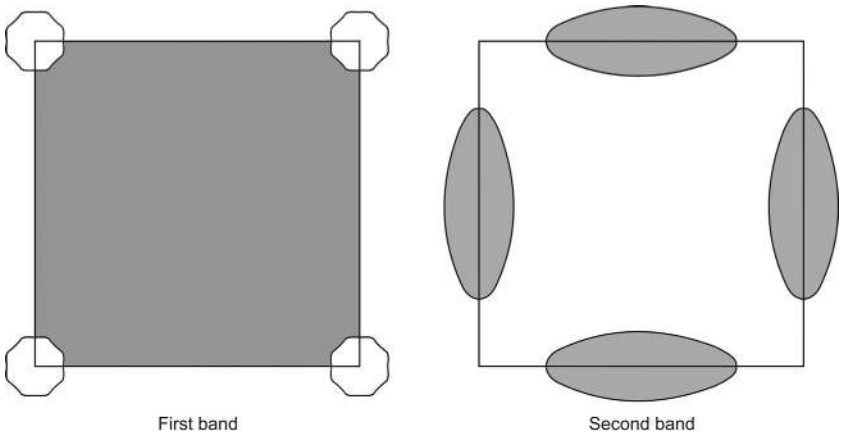

FIG. 13.15 The Fermi surface of the first and second energy bands in a square lattice for a two-dimensional nearly free-electron metal (in the periodic zone scheme).

$$\frac{k_F}{d} = \left(\frac{3}{\sqrt{2}\pi}\right)^{1/3} = 0.876 \tag{13.8}$$

From Eq. (13.8), it is evident that $k_F < d$. Hence, if the Na metal is treated as a free-electron metal, then the whole of the Fermi sphere will be well within the 1BZ as in Fig. 13.2. But, if Na is assumed to be a nearly free-electron metal, then there are zone boundary effects, that is, the bands bulge in the outward direction near the zone boundary and intersect it perpendicularly. Because of zone boundary effects, the FS of Na exhibits necks at the centers of the BZ faces (the points at which the FS reaches out to the zone boundary).

Consider nearly free-electron monovalent metals with fcc crystal structure, such as Cu, Ag, and others. Here the 1NN distance is $\sqrt{2}a$ and the atomic volume is $V_0 = a^3/4$. The reciprocal lattice of fcc is bcc and, therefore, the shortest reciprocal lattice vectors of Cu metal are $(2\pi/a)(\pm 1, \pm 1, \pm 1)$ and the faces of the 1BZ lie midway to the points $(2\pi/a)(\pm 1, \pm 1, \pm 1)$, etc. The distance of the zone face from the center of the 1BZ becomes $d = \sqrt{3}\pi/a$. Hence for monovalent Cu metal

$$\frac{k_F}{d} = \left(\frac{4}{\sqrt{3}\pi}\right)^{1/3} = 0.91 \tag{13.9}$$

Again in Cu, $k_F < d$ and the FS exhibits necks at the center of the BZ hexagonal faces due to the zone boundary effects. The FS for Cu in the reduced zone scheme is shown in Fig. 13.16. The figure shows two constant energy orbits: the first one is a belly orbit labeled as H_{100}, which should appear in the de Haas-van Alphen effect when a magnetic field **H** is applied along the [100] direction, and the second is a neck orbit labeled as N, which should appear with **H** along the [111] direction. Note that in Cu, d-electrons are well below E_F except for one d-subband. Therefore, the effect of the d-electrons on the FS is negligible. But, in general, the d-electrons give rise to strong and anisotropic localized potentials, which make the periodic lattice potential strong and anisotropic. As a result, the FS suffers large deviations from the nearly free-electron shape.

Problem 13.1

Show that in a monovalent metal with sc structure

$$\frac{k_F}{d} = \left(\frac{3}{\pi}\right)^{1/3} \tag{13.10}$$

Discuss the FS for such a metal.

13.6.2 Polyvalent Metals

Consider a divalent metal in the free-electron approximation. Using Eq. (9.19), the ratio k_F/d is given by

$$\frac{k_F}{d} = \frac{1}{d}\left(\frac{6\pi^2}{V_0}\right)^{1/3} \tag{13.11}$$

Therefore, for divalent metals with different structures, one can write

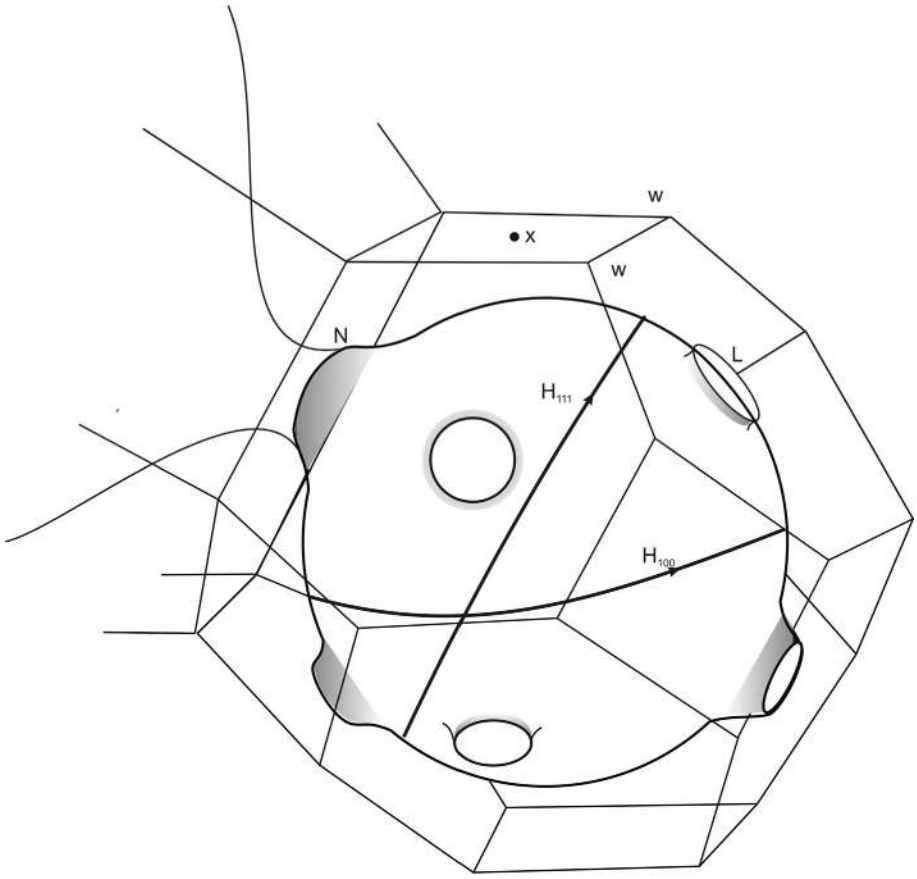

FIG. 13.16 The Fermi surface of the nearly free-electron metal Cu showing necks at the center of the zone faces. X and L are the symmetry points at the centers of the square and hexagonal faces, respectively, and W is the symmetry point at the corner of the face. *(After Burdick, G. A. (1963). Energy band structure of copper.* Physical Review, 129*, 138–150.)*

$$\begin{aligned}\frac{k_F}{d} &= \left(\frac{8}{\sqrt{3}\pi}\right)^{1/3} \text{ for fcc structure} \\ &= \left(\frac{3\sqrt{2}}{\pi}\right)^{1/3} \text{ for bcc structure} \\ &= \left(\frac{6}{\pi}\right)^{1/3} \text{ for sc stucture}\end{aligned} \tag{13.12}$$

Similarly, one can find the ratio k_F/d for trivalent metals in the free-electron approximation:

$$\begin{aligned}\frac{k_F}{d} &= \left(\frac{4\sqrt{3}}{\pi}\right)^{1/3} \text{ for fcc structure} \\ \frac{k_F}{d} &= \left(\frac{9}{\sqrt{2}\pi}\right)^{1/3} \text{ for bcc structure} \\ \frac{k_F}{d} &= \left(\frac{9}{\pi}\right)^{1/3} \text{ for sc structure}\end{aligned} \tag{13.13}$$

From Eqs. (13.12), (13.13) it is evident that $k_F > d$; therefore, in the polyvalent metals, the occupied bands extend to the higher-order BZs. As a result, the FS of polyvalent metals extends to the higher-order BZs. For example, Al, which is trivalent, is a nearly free-electron metal as is evident from its electron energy bands. The lower band exhibits 3s character, while the upper valence bands exhibit 3p character. Further, in Al, the lower 3s band is completely filled with 2N electrons, while the rest of the N valence electrons are distributed in the 3p bands.

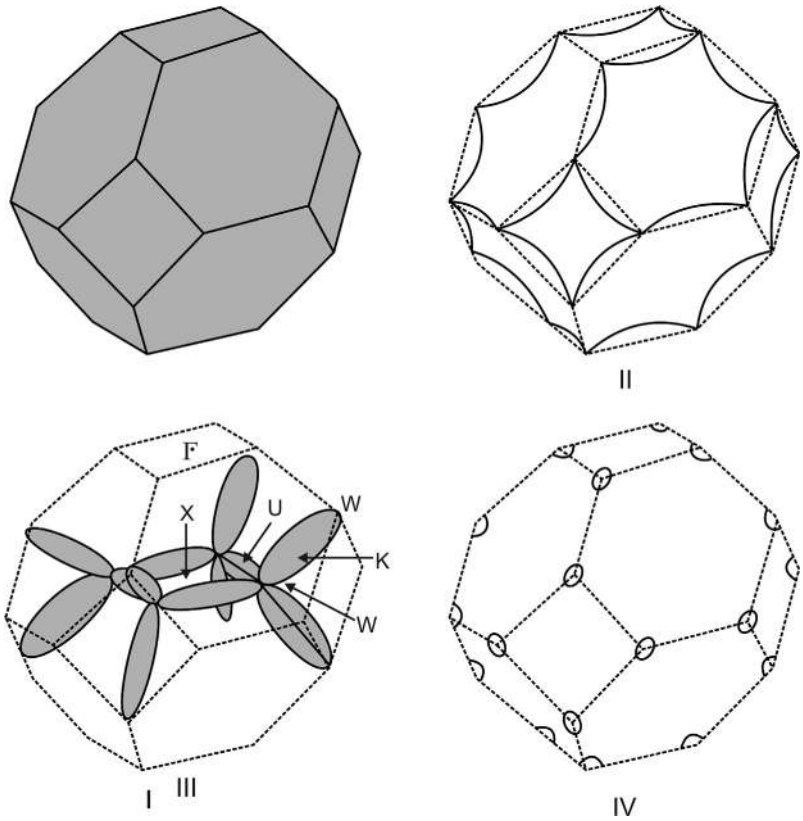

FIG. 13.17 The Fermi surface of Al metal in the free-electron model (Harrison, 1960). The first (I) band is completely full. In the second band (II) the region around the faces is full. In the third band (III) a complex region around the edges with many narrow areas is full. These narrow regions may be translated and put together to form a monster. In the fourth band there are small pockets around the W points that are full.

Harrison (1960) studied the FS of Al in the free-electron approximation, which extends to the 4BZ in the extended zone scheme (Fig. 13.17). It is evident that the first band is completely full with 2N electrons in it. The rest of the N valence electrons are distributed in the second, third, and fourth bands: in the second band the region around the zone faces is full, while in the third and fourth bands small electron pockets are formed around the edges and corners, respectively. The occupied region of the third band, when reduced to the 1BZ, forms a monster-like shape (see Fig. 13.17). The three-dimensional view of the FS of metals is complex and is still more complex for metals with geometry of low symmetry.

13.7 EXPERIMENTAL METHODS IN FERMI SURFACE STUDIES

A number of powerful experimental techniques have been developed for the study of the FS of metallic solids. Some of these methods are:

1. de Haas-van Alphen effect
2. Cyclotron resonance
3. Anomalous skin effect
4. Magnetoresistance
5. Ultrasonic propagation in magnetic fields

The de Haas-van Alphen effect and cyclotron resonance exhibit quantization of electronic states in the presence of a magnetic field. In these methods the effect of a uniform magnetic field on the electronic motion in **k**-space can be visualized. It is from this insight that the shape of the FS in **k**-space can be determined.

13.7.1 de Haas-van Alphen Effect

De Haas and Van Alphen, in 1931, discovered that, at low temperatures, the diamagnetic susceptibility χ_M of pure Bi shows periodic oscillations when plotted against the high values of an applied magnetic field **H**. These oscillations display a

remarkable periodicity when susceptibility is plotted against the inverse of magnetic field (Fig. 13.18). This effect has been used successfully in determining the extremal cross-sectional areas of the FS. It is a quantum mechanical effect arising from the quantization of the electron orbits in the magnetic field. It is noteworthy that more precise measurements exhibit similar oscillatory behavior in other properties also, such as conductivity and magnetic resistance. Very weak oscillations have also been observed in the high-field Hall effect.

We begin by considering the motion of electrons in a uniform magnetic field **H,** which according to Newton's second law of motion gives

$$\hbar \frac{d\mathbf{k}}{dt} = -\frac{e}{c}\mathbf{v} \times \mathbf{H} \tag{13.14}$$

According to Eq. (13.14) the electron will travel in an orbit with a shape determined by **v** and **H** in real space and the rate of change of **k** is a vector normal to **H**. Therefore, in **k**-space, the electron wave vector moves in an orbit with its plane normal to **H**. Integrating Eq. (13.14) one gets

$$\mathbf{k} = -\frac{e}{c\hbar}\mathbf{r} \times \mathbf{H} \tag{13.15}$$

This implies that the orbits in **k**-space and in real space are identical: **k**-space is obtained from real space by a rotation through $\pi/2$ about the axis of **H** and multiplication by a numerical factor e H/c ħ.

The orbits may be closed or open, but here we consider only the properties of the closed orbits. In a closed orbit, the electron wave vector **k** will execute a periodic motion in **k**-space and the frequency of this motion is called the cyclotron frequency. A convenient expression for the cyclotron frequency may be obtained by constructing two orbits in **k**-space in a plane perpendicular to **H** and having slightly different energies. Two such adjacent orbits are shown in Fig. J2 of Appendix J. The time period T of an electron orbit in a magnetic field is given by

$$T = \oint dt = \oint \frac{d\mathbf{r}}{\mathbf{v}} \tag{13.16}$$

where **v** is the velocity of the electron in a band with energy E in **k**-space and is given by

$$v = \frac{dr}{dt} = \frac{1}{\hbar}\frac{dE}{dk} = \frac{1}{\hbar}\frac{dE}{dk_\perp} \tag{13.17}$$

where $d\mathbf{k}_\perp$ is the normal distance in **k**-space between constant energy surfaces of energy E and E + dE. Substituting **v** from Eq. (13.17) into Eq. (13.16), we find

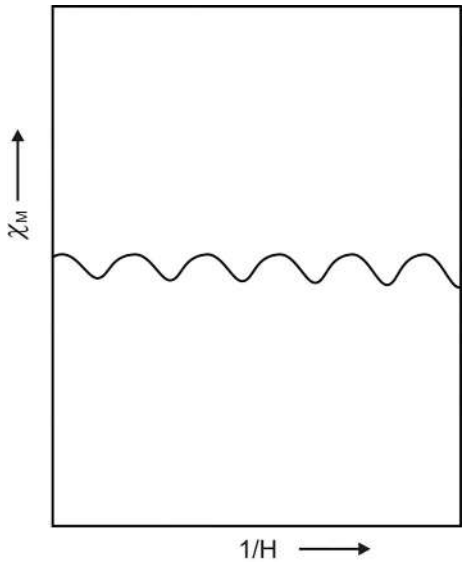

FIG. 13.18 The diamagnetic susceptibility of Bi as a function of 1/H at high magnetic field H.

$$T = \hbar \oint \frac{d\mathbf{r} \times d\mathbf{k}_\perp}{dE} = \frac{c\hbar^2}{eH} \oint \frac{|d\mathbf{k} \times d\mathbf{k}_\perp|}{dE} = \frac{c\hbar^2}{eH} \frac{dA_e}{dE} \tag{13.18}$$

Here $d\mathbf{k}$ is an infinitesimal change in the wave vector along the orbit in an infinitesimal time dt. Therefore, the term $\oint |d\mathbf{k} \times d\mathbf{k}_\perp|$ is simply the area dA_e between the two orbits in wave vector space. The cyclotron frequency is given by

$$\omega_c = \frac{2\pi}{T} = \frac{2\pi eH}{c\hbar^2} \frac{dE}{dA_e} \tag{13.19}$$

The derivative of the orbital area with respect to energy is taken at a constant component of $\mathbf{k}$ parallel to the magnetic field. The cyclotron frequency from Eq. (10.24) can be written as

$$\omega_c = \frac{eH}{m_c^* c} \tag{13.20}$$

where m_c^* is the effective cyclotron mass. Comparing Eqs. (13.19), (13.20), m_c^* can be written as

$$m_c^* = \frac{\hbar^2}{2\pi} \frac{dA_e}{dE} \tag{13.21}$$

So far, the discussion of electron motion has been classical. Even under such conditions, the Bohr correspondence principle provides the quantization condition as

$$\oint \mathbf{p} \cdot d\mathbf{r} = 2\pi\hbar \left(n + \frac{1}{2}\right) \tag{13.22}$$

The momentum of a free electron in the presence of a magnetic field changes as

$$\mathbf{p} \rightarrow \mathbf{p} - \frac{e}{c}\mathbf{A} \tag{13.23}$$

where $\mathbf{A}$ is the vector potential defined as

$$\mathbf{H} = \nabla \times \mathbf{A} \tag{13.24}$$

Substituting for $\mathbf{k}$ from Eq. (13.15) in Eq. (13.23) and then $\mathbf{p}$ in Eq. (13.22), we get

$$\oint \mathbf{H} \cdot (\mathbf{r} \times d\mathbf{r}) - \oint \mathbf{A} \cdot d\mathbf{r} = \frac{2\pi\hbar c}{e} \left(n + \frac{1}{2}\right)$$

Here the integral $\oint \mathbf{r} \times d\mathbf{r}$ gives twice the area of the orbit, so that $\oint \mathbf{H} \cdot (\mathbf{r} \times d\mathbf{r})$ is twice the magnetic flux Φ. The term $\oint \mathbf{A} \cdot d\mathbf{r}$ also gives magnetic flux Φ. Therefore, the above equation, in terms of the magnetic flux Φ, can be written as

$$\Phi = \frac{2\pi\hbar c}{e} \left(n + \frac{1}{2}\right) \tag{13.25}$$

Eq. (13.25) implies that the magnetic flux through an electron orbit in real space is quantized in units of $2\pi\hbar c/e$. The magnetic flux is given by $\Phi = H A_r$ where A_r is the area of the orbit in real space. We have seen before, in this section itself, that the radius of the orbit in $\mathbf{k}$-space is $eH/c\hbar$ larger than that of the orbit in $\mathbf{r}$-space. Therefore

$$A_e = \left(\frac{eH}{c\hbar}\right)^2 A_r \tag{13.26}$$

One should note that A_e represents the extremal cross-sectional area of the FS in a plane normal to the magnetic field $\mathbf{H}$. The extremal area is either a maximum or minimum area of the cross section of the FS; therefore, the derivative of A_e with respect to $\mathbf{k}$ must be zero at that point. Substituting the value of A_r, one gets the magnetic flux as

$$\Phi = \frac{c^2\hbar^2}{e^2 H} A_e = \frac{2\pi\hbar c}{e} \left(n + \frac{1}{2}\right)$$

From the above expression one gets

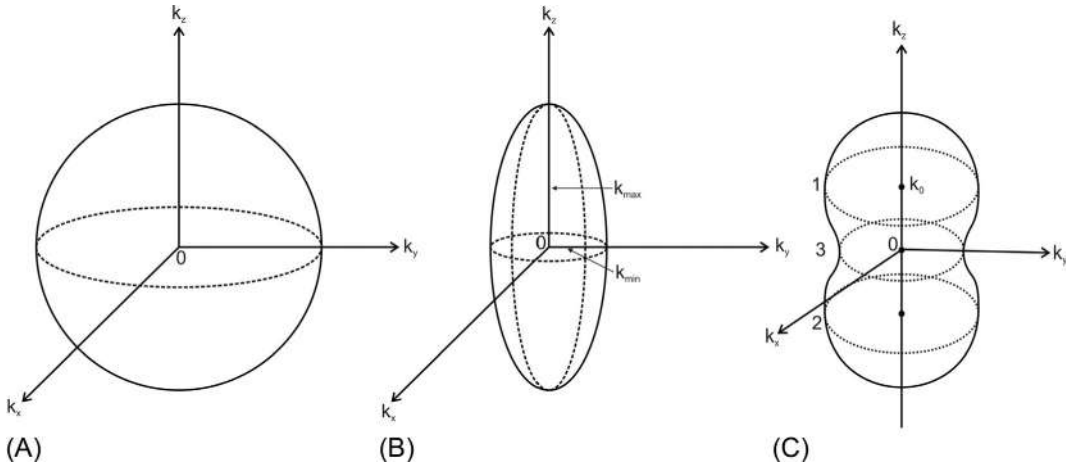

FIG. 13.19 The extremal areas of cross section in spherical, ellipsoidal, and dumbbell shaped Fermi surfaces.

$$A_e = \frac{2\pi eH}{c\hbar}\left(n + \frac{1}{2}\right) \tag{13.27}$$

This is known as the Onsager-Lifshitz quantization condition and this is the basis of the de Haas-van Alphen effect. Thus, the quantum condition allows only a certain discrete set of orbital areas in **k**-space. The size of these orbits is directly proportional to the magnetic field. The effect of a magnetic field has already been described in Chapter 10. In the absence of a magnetic field, the allowed states in two dimensions are shown in Fig. 10.7A, while they are shown in Fig. 10.7B in the presence of a magnetic field. Evidently the effect of the magnetic field is to create quantized circles in the **k**-space and cause the free electron states to condense into the nearest circle. These are the familiar Landau levels, as discussed in Chapter 10. The successive Landau levels correspond to successive values for the quantum number n. The reciprocal of the magnetic field, from Eq. (13.27), is given by

$$\frac{1}{H} = \frac{2\pi e}{A_e \hbar c}\left(n + \frac{1}{2}\right) \tag{13.28}$$

The reciprocal of the magnetic field induces fluctuations in the magnetic susceptibility. The period of oscillation is inversely proportional to the cross-sectional area of the FS. In three dimensions the allowed states lie in tubes in **k**-space each of which has constant cross section in the planes perpendicular to the magnetic field. Such sets of tubes or cylinders are shown in Fig. 10.5B. Each tube has been cut off at a constant energy surface corresponding to the FS.

In the determination of the FS, a magnetic field is applied at different angles to the axis of the single crystal and time period T is measured as a function of **H**. It then becomes possible to measure the extremal area of the FS normal to the direction of **H** using Eq. (13.28). The extremal areas for simple shapes of the Fermi surface are shown in Fig. 13.19. In a spherical Fermi surface there is only one extremal (maximum) area for all the directions of the **H** field and that is a circle having area πk_F^2 (Fig. 13.19A). In the case of an ellipsoidal Fermi surface with k_{max} and k_{min} as the major and minor axes, the magnitude and shape of the extremal area depends on the direction of the **H** field. If the **H** field is applied along the z-direction, then the extremal area is a circle with area πk_{min}^2 (see Fig. 13.19B). But if the **H** field is along the y-direction, the extremal area is an ellipse with area $\pi k_{max} k_{min}$. For a dumbbell-shaped Fermi surface, the extremal areas are shown in Fig. 13.19C. If the **H** field is applied in the z-direction, then there are three extremal areas: two circular orbits with maximum area (labeled as 1 and 2) and one circular orbit (labeled as 3) with minimum area. But if the **H** field is in the y-direction, then there is one extremal area having a dumbbell shape.

The oscillatory behavior of the magnetic susceptibility and other related properties can be explained as follows. The quantum condition produces a sharp oscillatory structure in the electron density of states, with its peak occurring at the energy corresponding to the extremal orbit satisfying the quantum condition. At the extremal orbit, the area of the portion of the tube is enormously enhanced as a result of the slow variation of the energy along the tube near the given orbit.

13.7.2 Cyclotron Resonance

The cyclotron resonance method makes use of the fact that, if an rf electric field is applied to a metallic solid, it penetrates at the surface by a small distance (skin depth). The Azbel-Kaner geometry is often employed for the study of cyclotron

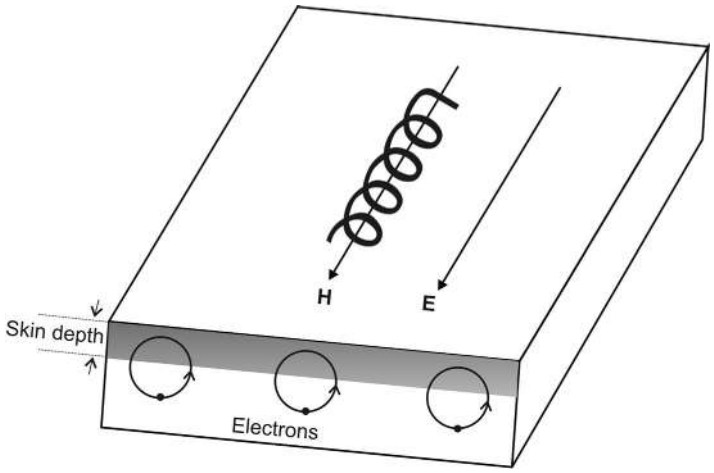

FIG. 13.20 The Azbel-Kaner geometry for cyclotron resonance in a metallic slab with **H** and **E** fields parallel to each other and in the same direction (longitudinal geometry). The circular motion of the electrons is shown in the front face of the metallic slab, which is perpendicular to **H** field. The shaded region shows the extent of penetration of the field inside the slab.

resonances in metals: here an rf electric field **E** and static magnetic field **H** are applied parallel to the surface of a metallic slab. In this geometry two types of studies are performed: first when **E** and **H** are perpendicular to each other (transverse geometry) and second when **E** and **H** are parallel to each other (longitudinal geometry). Fig. 13.20 shows the longitudinal geometry in which **E** and **H** are in the same direction. Note that if **E** and **H** are parallel but in opposite directions, then the direction of motion of the electrons is reversed. The shading in the figure near the surface of the solid indicates the penetration depth of the rf field. Under the combined effect of both the **E** and **H** fields, the electron moves in a helical path. Fig. 13.20 also shows the circular path of the electrons perpendicular to the direction of **H** in the front face of the metallic slab. The frequency of circular motion, called the cyclotron frequency, is given by Eq. (13.20). The time period T of the electron orbit is defined by

$$T = \frac{2\pi}{\omega_c} = \frac{2\pi m_c^* c}{eH} \tag{13.29}$$

The radius of the orbit of an electron in a magnetic field of 10 kilogauss is on the order of 10^{-3} cm, which is much larger than the skin depth at radio frequencies in a pure metal at low temperatures. Electrons in orbits, such as those shown in Fig. 13.20, will see the rf field only for a small part (near the top) of each cycle of their motion. The electrons are accelerated in each cycle if the phase of the electrons when they arrive in the skin depth part of each cycle is the same as that of the rf field. This will happen only when the frequency of the rf field ω is equal to an integral multiple of the cyclotron frequency, that is,

$$\omega = n\omega_c \tag{13.30}$$

Here n is an integer 1, 2, 3, … and it defines the harmonics of the cyclotron frequency. This is called the Azbel-Kaner resonance or cyclotron resonance and in this condition the electrons absorb the maximum energy. Substituting the value of ω_c from Eq. (13.20) into Eq. (13.30), we find

$$\omega = \frac{neH}{m_c^* c} \tag{13.31}$$

which gives

$$H = \frac{\omega m_c^* c}{ne} \tag{13.32}$$

One can express this resonance condition in terms of the extremal areas of cross section by substituting m_c^* from Eq. (13.21) into Eq. (13.32) to get

$$\frac{1}{H} = \frac{2\pi ne}{c\hbar^2 \omega} \frac{dE}{dA_e} \tag{13.33}$$

Fig. 13.21 represents the Azbel-Kaner cyclotron resonance spectrum for Cu metal at 4.2 K. The ordinate of the curve represents the derivative of the surface resistivity with respect to the field. In general, the electrons in different regions of the surface have different cyclotron frequencies. But the frequency that is most pronounced in absorption is the frequency

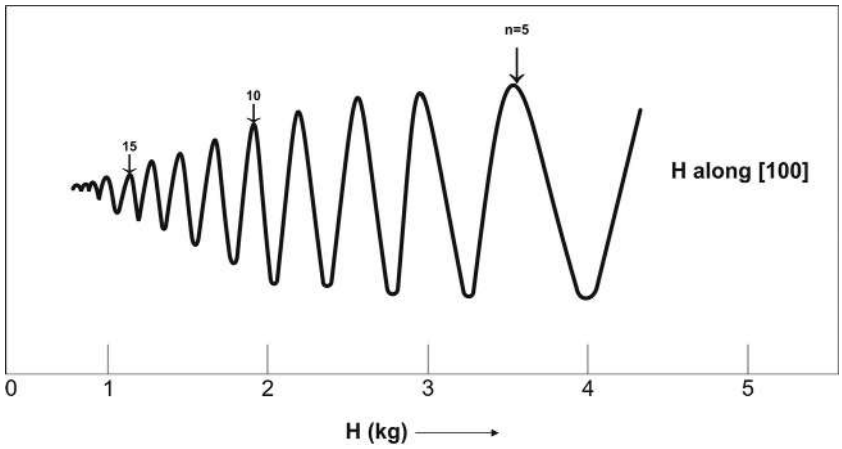

FIG. 13.21 Azbel-Kaner cyclotron resonance spectrum for Cu metal at 4 K. The upper crystal surface is cut along the (100) plane. *(After Haussler, P. & Welles, S. J. (1966). Determination of relaxation times in cyclotron resonance in copper.* Physical Review, 152*, 675.)*

appropriate to the extremal orbit in which the FS cross section perpendicular to **H** is maximum or minimum. Therefore, by varying the orientation of **H**, one can measure the extremal sections in various directions and reconstruct the FS. One can determine the various electronic properties and their oscillatory behavior in the same way as described in the de Haas-van Alphen effect.

REFERENCES

Harrison, W. A. (1960). Electronic structure of polyvalent metals. *Physical Review*, *118*, 1190–1208.

SUGGESTED READING

Altmann, S. L. (1970). *Band theory of metals*. New York: Pergamon Press.

Callaway, J. (1958). Electron energy bands in solids. F. Seitz, & D. Turnbull (Eds.), *Solid state physics* (pp. 100–212). Vol. 7(pp. 100–212). New York: Academic Press.

Cornwell, J. F. (1969). *Selected topics in solid state physics: Group theory and electronic energy bands in solids*. Amsterdam: North-Holland Publ. Co.

Cracknell, A. P., & Wong, K. C. (1973). *The Fermi surface: Its concept, determination and use in the physics of metals*. London: Clarendon Press.

FURTHER READING

Burdick, G. A. (1963). Energy band structure of copper. *Physical Review*, *129*, 138–150.

8
Fermi Surfaces and Metals

8.1. Folding of the Brillouin zone

8.1.1. 1D

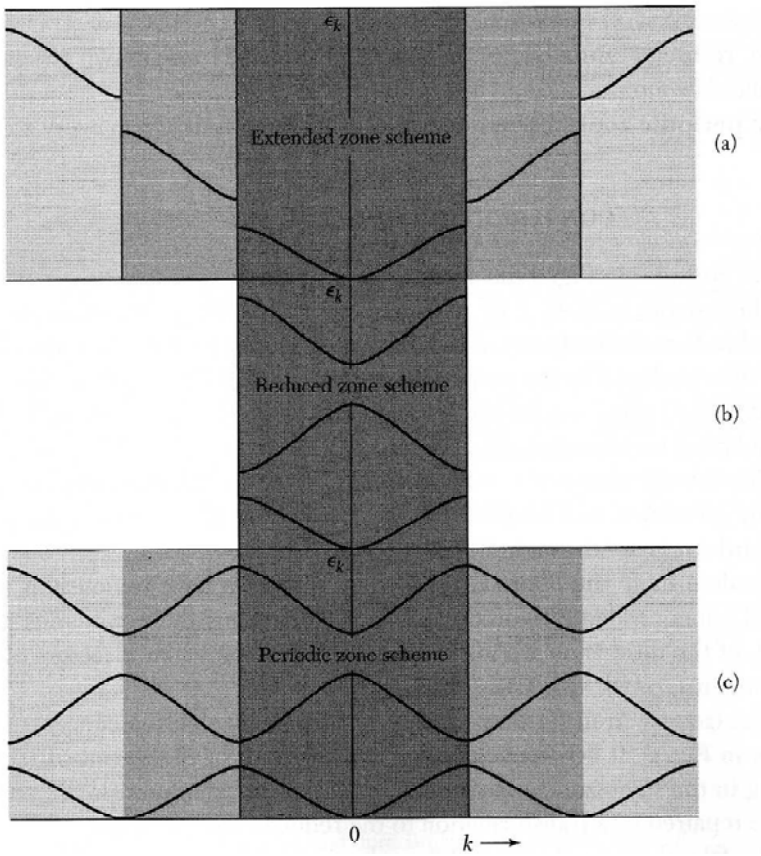

Fig. 1. Dispersion relation $\epsilon_n(k)$ shown in extended zone, reduced zone and periodic zone. (Figure 4 in text book page 225).

8.1.2. 2D

Let’s start by considering a very weak square lattice.

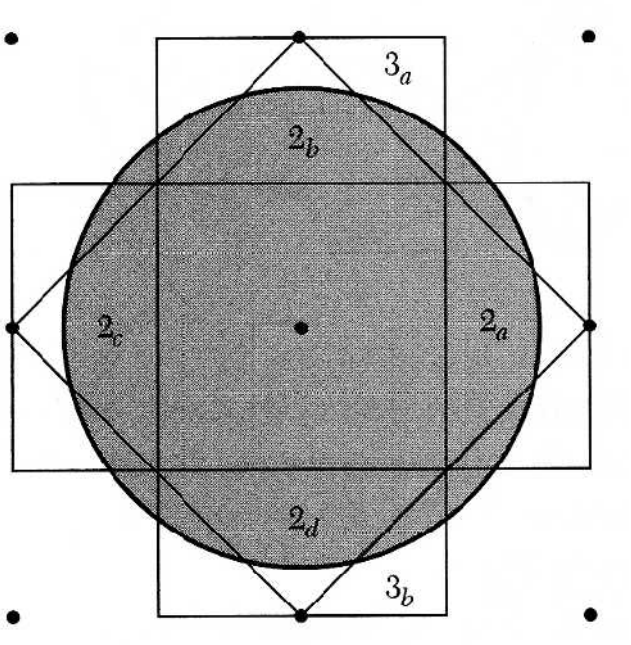

Fig. 2. The Fermi sea in extended zone (a square lattice). The solid lines show the zone boundaries. Here we assume that the lattice potential is very weak, so that the Fermi sea is pretty much a sphere (Figure 6 in text book page 227).

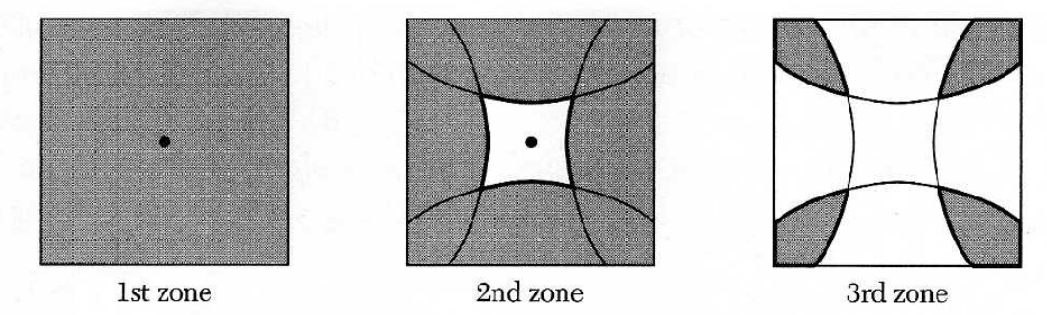

Fig. 3. The Fermi sea shown in the reduced zone. The first zone is fully filled, while the 2nd and 3rd zones are partially filled. The second zone has a hole pocket and the 3rd zone has a electron pocket. (Fig. 8, page 228).

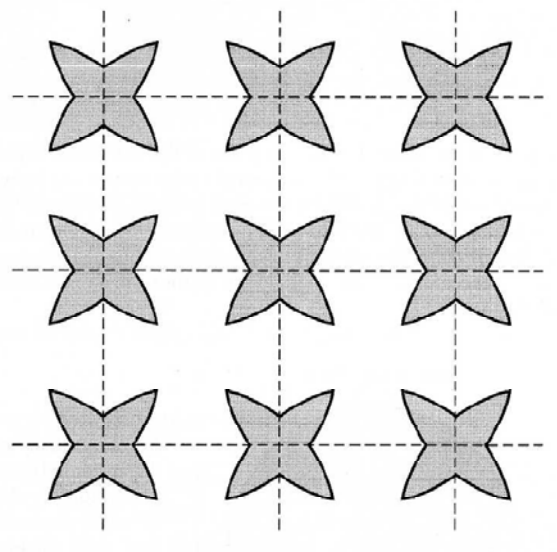

Fig. 4. Third zone (Fig 3.c) shown in the periodic zone. As we can see here, in the reduced zone, naively speaking, it seems that we have 4 disconnected dark regions (states filled by electrons). However, we need to keep in mind that the zone has a periodic structure. If we take into account the periodic structure, we find that in the 3rd zone here, the four seemingly disconnected regions are actually connected. They form one electron pockets.(Fig. 9 page 228)

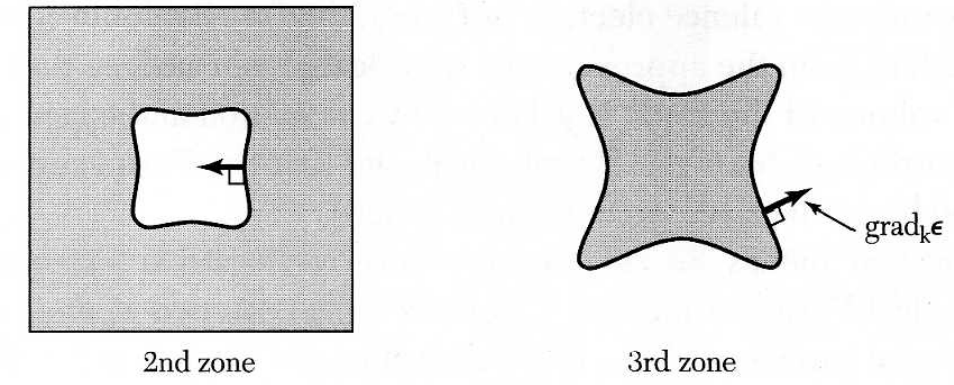

Fig. 5. If we turn on a weak lattice potential, the sharp corners of the Fermi surfaces will be rounded up and one can prove that when the Fermi surface crosses with a zone boundary, the Fermi surface must be perpendicular to the boundary.(Fig. 10 page 229)

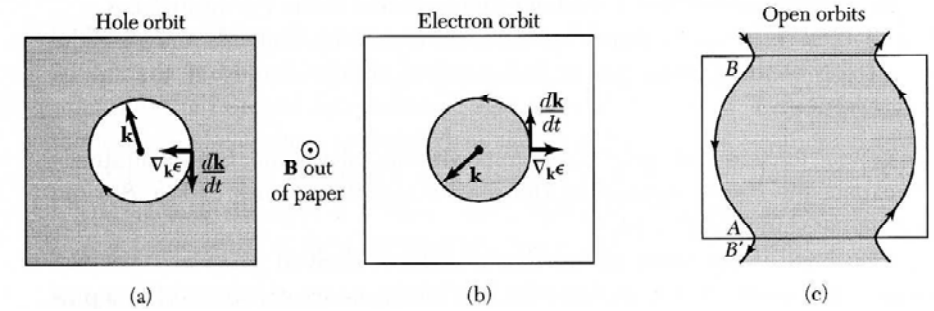

Fig. 6. (a) a partially filled band with one hole pocket (b) one electron pocket and (c) open orbitals.

For Fig. 6(b), we have a Fermi sea, which are formed by filling the states inside the Fermi surface using electrons. This filled region is known as an electron pocket and the Fermi surface here is known as an electron orbit.

For the case shown in Fig. 6(a), we have a almost fully-filled band. In some sense, it is exactly opposite to the case 6(b). Here, the Fermi surface enclose a region which is empty. For such a band, we can think the empty states as filled by “holes”. A hole is a missing electron. Since an electron has charge -e, a hole shall have charge +e (missing a charge -e means charge +e). A hole is also a Fermi with spin-1/2. The white region in Fig. 6(a), i.e. the empty states, can be considered as a Fermi sea filled by holes. This Fermi surface is known as a hole orbit. And the (white) region enclosed by the Fermi surface is known as a hole pocket. For this band, the conductivity are contributed by “holes”. Remember that in previous chapters, we discussed the Hall effect. The Hall coefficient is determined by the charge density. For electron pockets, the value is negative because electrons are negatively charged. For hole pockets, they give us a positive Hall coefficient, because the charge are carried by holes with positive charge.

Fig. 6(c) shows another possible case, where the Fermi surface doesn’t form a closed loop inside one zone. This Fermi surface is known as an open orbit.

It is possible to have multiple orbits in one zone and it could even be a combination of different types of orbits.

8.1.3. 3D

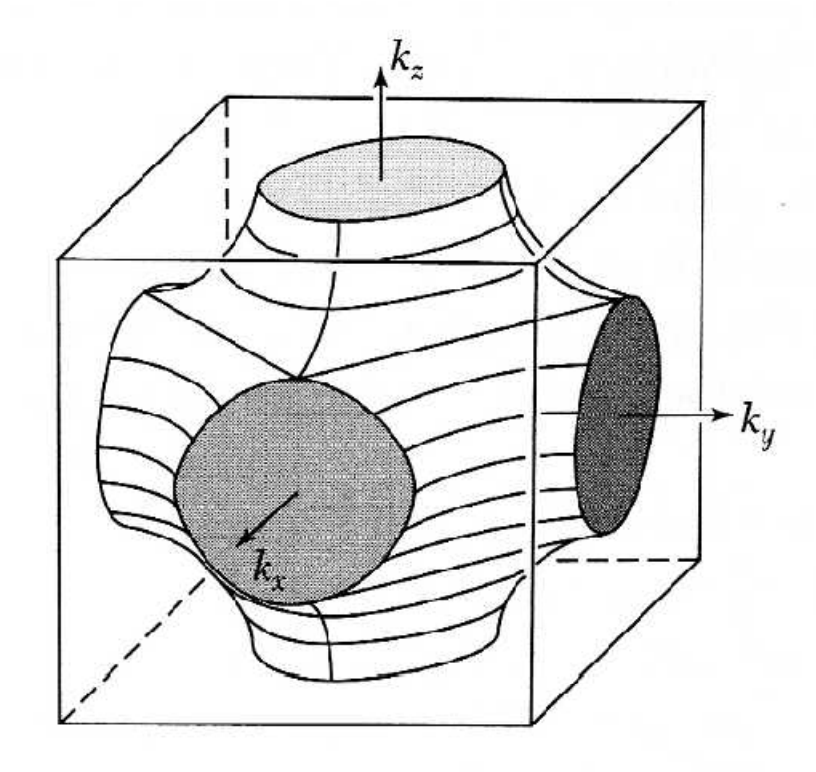

We can cut a plane in the 3D reduced zone. Depending on which plane we cut, we may find an electron orbital, a hole orbital or an open orbital in the figure above.

8.2. How to see the Fermi surface part I: ARPES: Angle-Resolved Photoemission Spectroscopy

- Setup: shoot light (photons) onto the material. When a photon hit a electron (collision) inside the sample, the electron may fly out of the sample (which is known as photoemission) and this electron will be picked up by an detector. The detector can distinguish electrons with different energy and momentum (including both the amplitude and the direction of the momentum, which is a vector). The detector counts the number of electrons which have the energy ϵ and the momentum $\vec{p}$.
- Basics idea: we know the energy and momentum of the photon and we can measure the energy and momentum of the out-coming electron. Using energy and momentum conservation, we can get the energy and momentum of the electron before it was hit by the photon. This tells us the relation between ϵ and p for an electron inside the material and thus we can get the dispersion relation and to construct the Fermi surfaces.

The energy conservation tells us that

$$E_p + \epsilon = E_{\text{final}} \tag{8.1}$$

where E_p is the energy of the photon (light), ϵ is the energy of an electron inside the material, and E_{final} is the energy of the electron coming out of the sample. E_p and E_{final} can be measures, so that we can determine ϵ

Similarly, we have momentum conservation for the x and y direction. When the electron flies out of the sample, it crosses the surface. When electron crosses the surface, it will lose some momentum along the z-direction. So the z momentum is NOT conserved, but the x and y directions are).

$$\vec{P}_{//\,p} + \vec{P}_{//} = \vec{P}_{//\,\text{final}} \tag{8.2}$$

Here, $\vec{P}_{//\,p}$ is the in plane components of the momentum of the photon, $\vec{P}_{//}$ is the in-plane momentum of the electron (inside the

material), and $\vec{P}_{//\,\text{final}}$ is the momentum of the final electron flying away from the sample.

Combining the information obtained above, we get the energy and momentum (in plane) of an electron. There are more complicated techniques that can provide us the z component of the electron. At the end of the day, we can get both ϵ and $\vec{P}$, so we get the dispersion relation $\epsilon\left(\vec{P}\right)$. And we can get the Fermi surface by requiring $\epsilon\left(\vec{p}\right) = \mu$.

Limitations of ARPES:

- It is a surface probe: light cannot go deep into a metal, so we can only measure the electronic properties near the surface of the sample. For some materials, surface is pretty much the same as bulk, but for some other materials it isn't the case. There, what we see in ARPES may not reflect the true properties of the material in the bulk. So one need to be very careful about it.
- ARPES needs a very clean and flat surface (easier for layered materials but not easy for many other materials).
- One can only measure the dispersion relation for $\epsilon \le \mu$. This is because we need to get one electron out of the sample from the quantum state with energy ϵ and momentum p. This means that we can only see occupied states in ARPES. If the state is empty ($\epsilon > \mu$), there is no electron, so we cannot see this state. This is also how μ is determined in ARPES experiments. (There are techniques which allow us to see energy above the Fermi energy).
- The momentum resolution for P_z is lower than P_x and P_y.

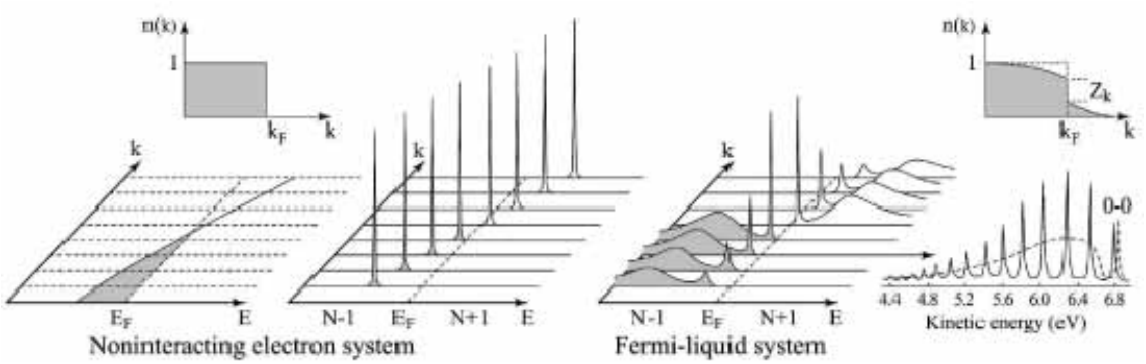

Fig. 7. Number of electrons received by the detector as a function of the momentum k and energy E. The l.h.s. shows the spectrum for free electrons. The r.h.s. shows the more realistic situation when we have interacting electrons. The locations of the peaks mark the dispersion relation $\epsilon(k)$. Figure from the webpage of the group lead by Z.X. Shen, Stanford University.

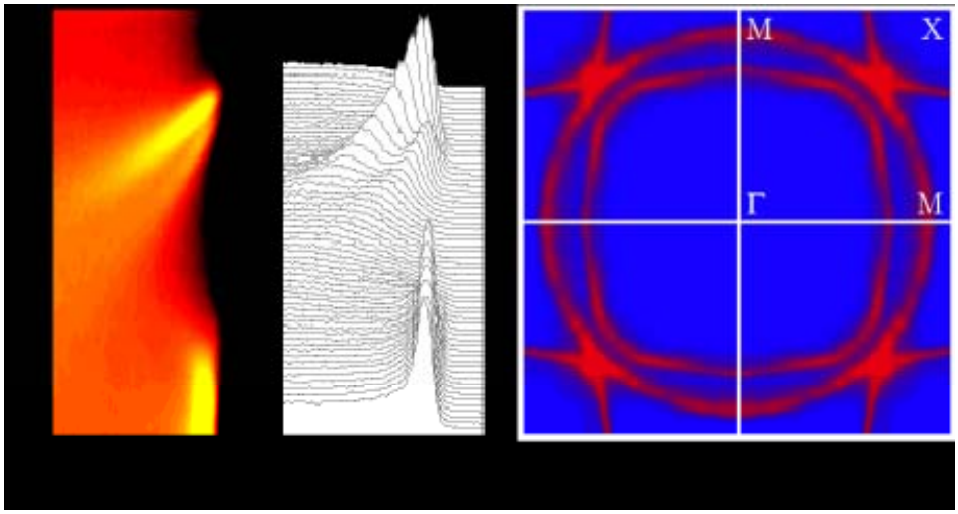

Fig. 8. Experimental data. The red circles shows the Fermi surfaces. Figure from the webpage of the group lead by Z.X. Shen, Stanford University.

8.3. De Haas-van Alphen oscillation

8.3.1. Classical mechanics

Consider an electron moving in 2D and we apply a magnetic field in the perpendicular direction (the z-direction). The Lorentz force is perpendicular to the direction of the velocity

$$\vec{F} = \frac{q}{c}\vec{v}\times\vec{B} \tag{8.3}$$

We know that in classical mechanics, when a force is perpendicular to the velocity, we will have a circular motion. The acceleration of a circular motion is

$$a = \frac{v^2}{r} = \frac{F}{m} = \frac{q}{m\,c}\,v\,B \tag{8.4}$$

So we have

$$v = \frac{q}{m\,c}\,B\,r \tag{8.5}$$

The period T is

$$T = \frac{2\,\pi\,r}{v} = \frac{2\,\pi\,r}{\frac{q}{m\,c}\,B\,r} = \frac{2\,\pi\,m\,c}{q\,B} \tag{8.6}$$

The angular frequency

$$\omega = 2\,\pi/T = q\,B/m\,c \tag{8.7}$$

8.3.2. Semi-classical approach

The second Law of Newton tells us that $\vec{F} = d\vec{P}\Big/dt$

$$\frac{d\vec{p}}{dt} = \frac{q}{c}\frac{d\vec{r}}{dt}\times\vec{B} \tag{8.8}$$

$$\frac{d\vec{r}}{dt} = \nabla_{\vec{P}}\epsilon\left(\vec{p}\right) \tag{8.9}$$

The second equation comes from the definition of the group velocity $\frac{dr}{dt} = v = \frac{d\omega}{dk} = \frac{\hbar\,d\omega}{\hbar\,dk} = \frac{d\epsilon}{dk}$

Combine the two equations above, we find that

$$\frac{d\vec{p}}{dt} = \frac{q}{c}\nabla_{\vec{P}}\epsilon\left(\vec{p}\right)\times\vec{B} \tag{8.10}$$

So $\frac{d\vec{p}}{dt}$ is always perpendicular to the direction of $\nabla_{\vec{P}}\epsilon\left(\vec{p}\right)$. $\nabla_{\vec{P}}\epsilon\left(\vec{p}\right)$ is the gradient of the energy. It is always perpendicular to the direction of the equal energy curve. So, we know that $\frac{d\vec{p}}{dt}$ is always along the direction of the equation energy curve.

By applying a magnetic field on a 2D electron gas. The electron moves along the direction of the equal energy curve. For $\epsilon > \mu$, there is no electron there. So we don't need to consider them. For $\epsilon < \mu$, all the states along the equal energy curve are occupied by electrons, so we don't need to consider them.

What matters is the Fermi surface where $\epsilon = \mu$.

8.3.3. Quantization condition for electrons at the Fermi surface

The Bohr-Sommerfeld quantization condition

$$\oint \vec{p}\cdot\vec{dr} = 2\pi\hbar\,(n+\gamma) \tag{8.11}$$

where n is an integer and γ is some fixed value, typically 1/2.

For a circular motion, this implies that

$$\oint \vec{p}\cdot\vec{dr} = \frac{2\pi\hbar}{\lambda}\oint dr = \frac{2\pi\hbar}{\lambda}\,2\pi r = 2\pi\hbar\,(n+\gamma) \tag{8.12}$$

If we ignore γ, which is unimportant for the discussion below, this condition implies that

$$\frac{2\pi r}{\lambda} = n \tag{8.13}$$

When we travel around the circle, we want the circumference being an integer times the wave length. If this condition is satisfied, the wave will have constructive inference when it travels around the circle.

Let's come back to the equation of motion

$$\frac{d\vec{p}}{dt} = \frac{q}{c}\frac{d\vec{r}}{dt}\times\vec{B} \tag{8.14}$$

So we have

$$\vec{p} = \frac{q}{c}\vec{r}\times\vec{B} + \text{constant} \tag{8.15}$$

The constant part is unimportant, since we can always redefine the origin (the point which we called $r = 0$) to absorb the constant into $\vec{r}$. So we have

$$\vec{p} = \frac{q}{c}\vec{r}\times\vec{B} \tag{8.16}$$

$$\vec{p}\times\vec{B} = \frac{q}{c}\left(\vec{r}\times\vec{B}\right)\times\vec{B} = \frac{q}{c}\left[\vec{B}\left(\vec{r}\cdot\vec{B}\right) - \vec{r}\left(\vec{B}\cdot\vec{B}\right)\right] = -\frac{q}{c}\vec{r}\,B^2 \tag{8.17}$$

$$\vec{r} = -\frac{c}{q}\frac{\vec{p}\times\vec{B}}{B^2} \tag{8.18}$$

$$d\vec{r} = -\frac{c}{q}\frac{d\vec{p}\times\vec{B}}{B^2} \tag{8.19}$$

$$\begin{aligned}\oint \vec{p}\cdot\vec{dr} &= -\frac{c}{q}\oint \vec{p}.\frac{d\vec{p}\times\vec{B}}{B^2} = -\frac{c}{qB^2}\oint \vec{p}.\left(d\vec{p}\times\vec{B}\right) = \\ &-\frac{c}{qB^2}\oint \vec{B}.\left(\vec{p}\times d\vec{p}\right) = -\frac{c}{qB}\oint\left(\vec{p}\times d\vec{p}\right) = -\frac{c}{qB}\hbar^2\oint\left(\vec{k}\times d\vec{k}\right) = -\frac{c}{qB}\hbar^2 S = 2\pi\hbar\,(n+\gamma)\end{aligned} \tag{8.20}$$

where S is the area enclosed by the Fermi surface in the k-space.

$$\frac{1}{B} = -2\pi\,(n+\gamma)\frac{q}{cS\hbar} \tag{8.21}$$

If we tune the magnetic field B and measures something (e.g. magnetization) as a function of $1/B$, we shall observe oscillations and the periodicity is

$$\Delta\left(\frac{1}{B}\right) = \frac{2\pi e}{\hbar c S} \tag{8.22}$$

This periodicity depends on the area of the electron/hole pockets. This is one standard technique to determine the sizes and number of pockets in a metal.

8.3.4. 3D (see extremal orbitals on page 248-249)

Assume k_B is the momentum along the direction of the magnetic field. At a fixed k_B, the intersection between the constant-k_B plane and the 3D Fermi surface gives us some orbit(s), which is a 1D curve. Depending on the value of k_B, area enclosed by this orbit changes.

Q: The periodicity depends on the size of the orbit $\Delta\left(\frac{1}{B}\right) = 2\pi\hbar\frac{e}{cS}$. Which orbit should we use here to determine S?

A: The orbits with $\frac{d\epsilon}{dk_B} = 0$ are called the extremal orbits. The periodicity of the quantum oscillations is determined by the area of these extremal orbitals. If the magnetic field is along the high symmetry direction, these extremal orbitals are often the largest and smallest orbitals. They typically give two different periodicities (one from the largest orbit and the other from the smallest one). So the magnetization as a function of 1/B shows oscillations with two periodicities (similarly to the superposition of two waves with different wavelength).

8.4. tight-binding approximation

Consider electrons tightly bind to nucleons. For this case, we start from a single site and then treat the kinetic energy as hopping from one site to another near-by site.

For one site, we can use the atomic orbitals to mark each quantum state (s state, p state, ...). Assuming that different quantum states have very different energies, so that they don't talk much to each other. Within this assumption, we can focus on one quantum state (per site) and ignore all others. Assume that this quantum state is $|n\rangle$ for site n.

In a lattice, an electron can tunnel through the potential barrier (quantum tunneling) to another nearby site, and the tunneling can be described by the following Hamiltonian

$$H = -t\sum_n\left(|n\rangle\langle n+1| + |n+1\rangle\langle n|\right) \tag{8.23}$$

Here, we consider a 1D crystal, where n is the site index $n = 1, 2, \ldots, N$. The coefficient $(-t)$ is the tunneling amplitude and here we only consider tunnelings from one site to its neighbor.

Define

$$|k\rangle = \frac{1}{\sqrt{N}}\sum_n e^{-ink a}\left|n\right\rangle \tag{8.24}$$

where a is the lattice constant. The inverse transformation is

$$|n\rangle = \frac{1}{\sqrt{N}}\sum_k e^{ink a}\left|k\right\rangle \tag{8.25}$$

$$H = -t\sum_n\left[\left(\frac{1}{\sqrt{N}}\sum_k e^{ink a}\left|k\right\rangle\right)\left(\frac{1}{\sqrt{N}}\sum_{k'}\left\langle k'\right| e^{-i(n+1)k' a}\right) + \left(\frac{1}{\sqrt{N}}\sum_k e^{i(n+1)k a}\left|k\right\rangle\right)\left(\frac{1}{\sqrt{N}}\sum_{k'}\left\langle k'\right| e^{-ink' a}\right)\right] = -t\sum_k\sum_{k'}\left(\frac{1}{N}\sum_n e^{in(k-k')a}\right)\left(e^{-ika} + e^{ik' a}\right)\left|k\right\rangle \tag{8.26}$$

$$\left\langle k'\right| = -t\sum_k\sum_{k'}\delta_{k,k'}\left(e^{-ika} + e^{ik' a}\right)\left|k\right\rangle\left\langle k'\right| = -t\sum_k\left(e^{-ika} + e^{ika}\right)\left|k\right\rangle$$

$$\langle k| = \sum_k -2\,t\cos(k\,a)\,|k\rangle\langle k|$$

It is easy to check that

$$H\,|k\rangle = -2\,t\cos(k\,a)\,|k\rangle \tag{8.27}$$

so |k⟩ is an eigenstate of the Hamiltonian and the corresponding eigen-energy is $\epsilon(k) = -2\,t\cos k\,a$ with $-\pi/a < k < \pi/a$. This is one energy band.

The bottom line: If the atomic states are separated far from each other in energy (the energy difference is much larger than *t*), there is a one-to-one correspondence between atomic states in an atom and the energy bands. One atomic state (in each atom) gives us one band and one band comes from one atomic states. If the band comes from a s-orbital in an atom, we call it an s-band, p-orbitals form a p-band, etc.